HHS Public Access

Author manuscript

Regen Eng Transl Med. Author manuscript; available in PMC 2019 September 01.

Published in final edited form as:

Regen Eng Transl Med. 2018 September ; 4(3): 120–132. doi:10.1007/s40883-018-0054-2.

Cooperative Effects of Vascular Angiogenesis and Lymphangiogenesis

Tatsuya Osaki[1], **Jean C. Serrano**[1], and **Roger D. Kamm**[1,2,3]

[1]Department of Mechanical Engineering, Massachusetts Institute of Technology, Cambridge, MA, USA

[2]Department of Biological Engineering, Massachusetts Institute of Technology, Cambridge, MA, USA

[3]BioSystems and Micromechanics (BioSyM), Singapore-MIT Alliance for Research and Technology, Singapore, Singapore

Abstract

In this study, we modeled lymphangiogenesis and vascular angiogenesis in a microdevice using a tissue engineering approach. Lymphatic vessels (LV) and blood vessels (BV) were fabricated by sacrificial molding with seeding human lymphatic endothelial cells and human umbilical vein endothelial cells into molded microchannels (600 μm diameter). During subsequent perfusion culture, lymphangiogenesis and vascular angiogenesis were induced by addition of phorbol 12-myristate 13-acetate (PMA) and VEGF-C or VEGF-A characterized by podoplanin and Prox-1 expression. The lymphatic capillaries formed button-like junctions treated with dexamethasone. To test the potential for screening anti-angiogenic (vascular and lymphatic) factors, antagonists of VEGF were introduced. We found that an inhibitor of VEGF-R3 did not completely suppress lymphatic angiogenesis with BVs present, although lymphatic angiogenesis was selectively prevented by addition of a VEGF-R3 inhibitor without BVs. To probe the mechanism of action, we focus on matrix metalloproteinase (MMP) secretion by vascular endothelial cells and lymphatic endothelial cells under monoculture or co-culture conditions. We found that vascular angiogenesis facilitated lymphangiogenesis via remodeling of the local microenvironment by the increased secretion of MMP, mainly by endothelial cells. Applications of this model include a drug screening assay for corneal disease and models for tumorigenesis including lymphatic angiogenesis and vascular angiogenesis.

Keywords

lymphangiogenesis; angiogenesis; microdevice; 3D in vitro model; MMP

Corresponding author: Roger D. Kamm, **Tel:** (617) 253-5330, rdkamm@mit.edu.

Authors declared no competing interests.

Author contributions

T.O., J.C.S, and R.D.K conceived and designed the study. T.O conducted the experiments and analyzed the data. T.O., J.C.S., and R.D.K wrote the manuscript.

Introduction

Vascular angiogenesis (VA) and lymphangiogenesis (LA), the formation of new blood and lymphatic vessels from existing ones, respectively, have attracted attention over several decades in a wide range of fields such as cancer metastasis, tissue engineering, wound healing, and corneal transplantation [1–3]. In particular, because VA and LA play a major role in metastatic cancer and induce corneal transplant rejection along with the critical inflammation [4] due to an excessive immune response, the suppression of both phenomena by anti-angiogenic drugs [5, 6] has become an attractive alternative to treat these diseases. Although the mechanisms of VA have been extensively explored [7] [8] [9], studies of LA are relatively rare [2]. In addition, recent studies have shown that interactions between VA and LA prove mutually beneficial in cases such as corneal inflammation and various types of tumor [10, 11]. Moreover, lymph node metastasis has been documented to occur in the presence of new vessels created by VA to deliver sufficient oxygen [12]. Therefore, the development of an *in vitro* model of both VA and LA is essential in order to understand the interaction between both phenomena for various medical applications.

Two-dimensional (2D) and 3D angiogenesis models have been previously developed using many approaches [13–16]. For instance, in typical 2D sprouting assays, vascular endothelial cells (VECs) are embedded in ECM as a sandwich culture, and VA is assessed by observing tube formation [14]. In an alternative approach, encapsulation of VEC spheroids [17] and VEC-coated beads [18] in hydrogel has also been used to investigate the potential of VA and the efficacy of anti-angiogenic drugs. However, these approaches have limitations for such studies. In addition, to the difficulty quantifying sprouting activity, these platforms poorly recapitulate the native vascular structure and lack continuous perfusability, both of which are imperative physiological factors for VA and LA.

With the advent of microfluidics, many of these limitations have been addressed and eliminated [16, 19]. These *in vitro* microfluidic models have already been employed to investigate the mechanism of VA and for drug screening of anti-angiogenic factors with high throughput capabilities, while incorporating biomimetic cues such chemical gradients and mechanical stimuli in a tightly controlled 3D microenvironment. In these models, however, most have studied VA alone using either vascular endothelial cells or endothelial progenitor cells [19]. Recently, several *in vitro* LA models have been published [20, 21]. Despite this, there are few *in vitro* models that combine both VA and LA in the same extracellular matrix with a perfusable vasculature to mimic the tumor microenvironment [22], which can evaluate sprouting quantitatively. Because blood vascular endothelial cells (VECs) and lymphatic endothelial cells (LECs) share common molecular and functional traits, it can be difficult to distinguish between blood vessels and lymphatic vessels [23]. Nevertheless, LECs and VECs have distinct molecular and physiological behaviors, which can be identified by their gene expression profiles (e.g., LYVE-1, podoplanin, and Prox-1), functional characteristics [24], and morphological intercellular junctions.

Herein, we describe a 3D *in vitro* model existing of blood vessels and lymphatic vessels in collagen gel to investigate LA and VA simultaneously. We engineered the two vessel types by seeding human VEC and human LEC into separate microchannels in a collagen gel.

Sequentially, VA and LA were induced during continuous perfusion by the addition of VEGF-A or VEGF-C and phorbol 12-myristate 13-acetate (PMA) which is a strong inducer of sprouting [25] [26]. To characterize lymphatic and blood vessels, immunofluorescent staining was performed for junctional, surface, and transcriptional proteins including (podoplanin and Prox-1) and lymphatic specific junctions can be visualized by the staining of VE-cadherin and distinguished by the pattern of their expression at cell-cell junctions. In addition, to prove that this culture platform can be applied to study inhibition of either LA or VA for tumorigenesis and corneal inflammation, we demonstrated the influence of inhibitors of VEGF-A, B, and C to this model and MMP activity in both LA and VA.

Materials and Methods

Materials and reagents

Materials used for fabrication of the culture chamber were obtained from the following commercial sources: glass capillary (diameter, 600 μm; length, 3.2 cm) from Hirschmann Laborgeräte, Germany; poly (methyl methacrylate) plates from Astra products, USA. Human umbilical vein endothelial cells (HUVECs, CC-2517A), human neonatal dermal lymphatic microvascular endothelial cells (HMVEC-dLy-Neo, CC-2812), endothelial basal medium (EBM-2, CC-3156) and SingleQuots growth supplement (CC-4176) from Lonza, Switzerland; type I collagen and 10x Ham's F12 medium (Cellmatrix Type I-A) from Nitta Gelatin, Japan; vascular endothelial growth factor-A (VEGF-A) and VEGF-C from PeproTech, USA; ZM306416, Cabozantinib and SAR131675 from selleckchem, USA; MMP-2/MMMp-9 inhibitor (Abcam, ab145190); All other chemicals were purchased from Sigma, USA unless otherwise indicated.

Cell culture

HUVEC and HMVEC-dLy-Neo (LEC) were subcultured with endothelial growth medium (EGM2-MV) used at passage 5 for experiments. For inducing LA and VA, VEGF-A or C (10 ng/ml, 25 ng/ml and 50 ng/ml) and phorbol 12-myristate 13-acetate (100 ng/ml, PMA) were added to the EGM2-MV medium. All cells were cultured at 37°C with 5% CO_2 in a humidified incubator.

Device fabrication

An acrylic culture chamber was used, fabricated from four acrylic plates (thickness: 2 mm) and one glass plate (No.1 glass, thickness; 0.13-0.16 mm) using biocompatible glue. The end wall plates have 4 holes 600 μm in diameter separated by 1000-μm. All acrylic plates were cut using a CO_2 laser (Laser Cutter Epilog Fusion 40). The volume of the chamber is ~250 μl and its internal height, width, and depth were 10 mm, 12 mm, and 3 mm, respectively. To sterilize the culture chamber, it was immersed in 70% ethanol for 30 min, then dried under UV light for > 30 min.

Formation of lymphatic and vascular vessels

To create perfusable and fully surrounded channels in a collagen gel, 3D cylindrical microfluidic channels were cast using one or two glass rods that were inserted into the acrylic culture chamber (Fig. 1A). Then, collagen type I pre-mixture (400 μl of 3.0 mg/ml

collagen solution, 50 μl of 10x Ham's F12 medium, and 50 μl of reconstitution buffer (2.2 g $NaHCO_3$ in 100 ml of 0.05 N NaOH and 200 mM HEPES) was injected into the device, yielding a final collagen solution of 2.4 mg/ml. After 15 min incubation at 37°C for polymerization, the glass rods were removed. Then, LEC and/or VEC cell suspension medium (1×10^7 cell/ml in EGM2-MV) were injected into the microchannels. To improve cell adhesion, the culture chambers were inverted several times over 30 min (Fig. 1). After 24 h, EGM2-MV was replaced with EGM2-MV supplemented with PMA (100 ng/ml) and VEGF-C (1, 5, 10 and 50 ng/ml) in order to induce LA and VA. For perfusion culture, 24 h after seeding, a peristaltic pump was connected to the inlets of the chamber. The flow rate in each channel was set to the same value, 150 μL/min, producing a shear stress of ~ 0.18 Pa (~1.8 dyn/cm^2). To stabilize the vascular and lymphatic vessels, dexamethasone was added to the EGM2-MV medium.

Measurement of orientation in microchannels

The alignment of LECs and VECs in microchannels were quantified by determining the orientation of cells on the channel wall by Fast Fourier transform (FFT) [27] [28]. FFT images contained pixels distributed in a pattern, which reflect the degree of fiber orientation. Orientation angle was quantified from the mean intensity of the FFT images using the IMAGE J plugin (OrientationJ). The angle (θ) was then determined relative to the vessel axis in the flow direction and was used as an indicator of the level of alignment of cells.

Application of anti-LA and VA agents

To demonstrate the potential for drug testing to inhibit VA or LA, the VEGF receptor antagonists (10 μM ZM306416, 10 μM Cabozantinib and 10 μM SAR131675) and anti-inflammatory drug (10 μg/ml dexamethasone) was applied in the presence of VEGF-A and VEGF-C (25 ng/ml) to the lymphatic and blood vessels.

Immunofluorescent staining

To visualize LEC and VEC sprouting, cells in the device were fixed with 4% paraformaldehyde in Dulbecco's Phosphate-Buffered Saline with Ca_{2+} and Mg^{2+} ($DPBS^{++}$) for 20 min, treated with 0.2% Triton X-100 for 5 min, then treated with 1% bovine serum albumin (BSA) in $DPBS^{++}$ for blocking. Cells were then incubated with the PE-conjugated anti-human podoplanin antibody (Biolegend, 1:200) and anti-Prox-1 antibody (Abcam, 1:100) and anti-VE-cadherin (CD144) antibody (Biolegend) for 2 h at room temperature. Secondary antibodies were incubated with Alexa Fluor 488 conjugated goat anti-Rabbit IgG(H+L) and Alexa Fluor 555 conjugated goat antimouse IgG(H+L) for 2 h. F-actin was stained with Alexa Fluor 488 phalloidin (Cytoskeleton, Inc., Denver, CO, USA) and DAPI for 20 min at room temperature, followed by three washes in $DPBS^{++}$. Cells were observed using a phase contrast microscope (Axiovert 200, Zeiss, Germany) and a confocal laser scanning microscope (FV-1000, Olympus, Japan).

Quantification of mRNA by RT-PCR

To measure the biological activity of LEC and VEC, total RNA was isolated from tissues by incubation with TRIzol reagent (Life Science) to dissolve the collagen gel. Reverse

transcription was performed using SuperScript VILO cDNA synthesis kit (Invitrogen). Primers used; *VEGF-R3* forward: TGC ACG AGG TAC ATG CCA AC, *VEGF-R3* reverse: CTG CTC AAA GTC CTC ACG AA, *Prox-1* forward: AAA GGA CGG TAG GGA CAG CAT, *Prox-1* reverse: CCT TGG GGA TTC ATG GCA CTA A, *ORAI-1* forward: GGA CGC TGA CCA CGA CTA C, *ORAI-1* reverse: GGG ACT CCT TGA CCG AGT T, GAPDH forward: AAT GGA CAA CTG GTC GTG GAC, GAPDH reverse: CCC TCC AGG GGA TCT GTT TG, were purchased from integrated DNA technology. Real-time RT-PCR was performed with an Applied Biosystems 7900HT Fast Real-Time PCR System, using SYBR Premix Ex Taq (Takara). mRNA of glyceraldehyde 3-phosphate dehydrogenase (GAPDH) as housekeeping gene set to 100% was used as the internal standard in all experiments. The RT-PCR experiment was repeated at least 3 times for cDNA prepared from at least three batches.

Quantification of sprouting length

Lymphangiogenesis (LA) of LEC and vascular angiogenesis (VA) of HUVEC in a collagen gel were observed using confocal laser microscopy, and the capillary length and sprouting branch number were quantified using image analysis software (IMARIS, Bitplane, Switzerland). For 3D rendering, acquired high-resolution confocal z-stacks were represented as isosurface renderings. Total capillary length, sprouting area, and single cell migration were quantified from the reconstructed 3D image using cell counting module and a filament tracer module of the IMARIS software package in combination with Image J.

MMP array assay and ELISA measurement

To screen for MMP activity, an MMP array assay was conducted using a human MMP antibody array kit (Abcam, ab134004), targeting MMP-1, 2, 3, 8, 9, 10, and 13 and TIMP-1, 2, and 4. To quantify the concentrations of MMP-2 and MMP-9, human MMP-2 and MMP-9 ELISA kits (Raybiotech, ELH-MMP2-1, ELH-MMP9-1) were used. Samples were diluted 10 times before measurement.

Characterization of collagen fibers using reflection confocal microscopy

To visualize collagen gel fibers, confocal microscopy was used in reflection confocal mode. Autofluorescence of collagen gel fibers in the microdevice was imaged through a 488-nm band illuminated through a high-pass filter by a 559-nm laser. Each image slice is 0.5 μm thick and 100 images were typically obtained. These were used to construct fully 3D images and maximum intensity projections (MIPs). Fiber density was calculated from a binary image of the MIPs using Image J.

Statistical analysis

The values reported corresponding to an average value over a minimum of 3 independent experiments. Data are presented as mean values ±SD. Comparisons were performed using one-way ANOVA tests with pairwise comparisons Tukey-Kramer *post hoc.* **p <0.05, * p <0.01. The statistical tests were performed using JMP pro (SAS Institutes Inc.).

Results

Formation of lymphatic vessel (LV) and perfusion culture

Experiments were first conducted with LECs alone using a single glass rod. In these, LA was induced within 3 days of culture in the presence of VEGF-C and PMA. After 10 days, sprout length reached approximately 500 μm. Although cells were exposed to long-term perfusion, the lumen structure of the LEC-seeded channel maintained its original cylindrical cross-section and the cells remained attached to the entire channel surface (Fig. 2C). Interestingly, single LECs could be observed breaking loose and migrating away from the channel, more so than for HUVECs. The sprouts were extensive with small lumens created by LA (Fig. 2B-E and Supplementary Fig. 1). In addition to this tendency, the expression of podoplanin was inhomogeneous and localized, especially along the sprouts (stalk cells).

Quantitative PCR showed that the expression of VEGF-R3 and Prox-1 which are typical LV markers, as well as calcium release-activated calcium modulator (ORAI1) increased with perfusion culture over time (D1 vs. D10) (Fig. 2F). In addition, we confirmed that high concentrations of VEGF-C (50 ng/ml) strongly induced LA. LECs exhibit a low sprouting potential compared to HUVEC in mono-culture at low concentrations of VEGF-C with PMA (Supplementary Fig. 2A, C). At higher concentrations of VEGF-C, LA attained levels comparable to that of VA (Supplementary Fig. 2B). Moreover, LEC did not significantly respond to the addition of high concentrations of VEGF-A in terms of sprout length (Supplementary Fig. 2B).

Lymphatic vessel and blood vessel co-culture and induction of lymphangiogenesis (LA) and vascular angiogenesis (VA)

To create both lymphatic and blood vessels in the same gel, two glass rods were fixed parallel to each other in the culture chamber, creating two cylindrical microchannels. LECs and HUVECs were injected into neighboring channels sequentially (Fig. 3A), resulting in the formation of a lymphatic vessel and a blood vessel in the same collagen gel (Fig. 3B). During perfusion through both channels, VA and then LA can be observed. Sprouting length of HUVECs in the presence of VEGF-C (10 ng/ml) and PMA was greater than the length of LECs (Fig. 3B, D). After 7 days of perfusion culture, HUVECs and LECs approached each other but did not anastomose. Moreover, the diameter of VA sprouts was significantly larger than the LA sprouts (Fig. 3E). Immunostaining of podoplanin and Prox-1, a mature lymphatic marker, showed that both sprouting structures could be cultured and characterized separately (Fig. 3F). Treating the co-culture with different concentrations of VEGF-C, we found no response from HUVECs but the sprouting length of LECs increased in a dose-dependent manner (Fig. 3G). In contrast, single cell migration of LECs was not influenced by VEGF-C concentration (Fig. 3H).

Characterization of lymphatic junctions

One of the specific differences between lymphatic vessels and blood vessels is the pattern produced by the intercellular adherens junctions. LECs have discontinuous button-like junctions in the lymphatic capillaries, unlike the continuous zipper-like junctions found in collecting lymphatic vessels and all blood vessels *in vivo* [29]. This button-like junction acts

as the primary valve, regulating flow and immune cell entry into the lymphatics [30]. We used immunofluorescence to examine the VE-cadherin distribution in adherens junctions in the lymphatic and blood vessels and their sprouts. VE-cadherin was tightly expressed on the boundary in both types of large vessel, forming zipper-like junctions (Fig. 4A). In our model, both LEC and EC in lymphatic capillaries and blood capillaries formed zipper-like junctions (Fig. 4B), which is associated with low permeability. Despite these tendencies, however, the structures observed in the LEC still differ considerably from those seen *in vivo.*

To enhance network stability, promote physiologically relevant structures, and reduce inflammation caused by the addition of VEGF-C, dexamethasone was introduced 48 h after LA and VA; it is known that dexamethasone reduces inflammation by inhibiting the MAK and NF-κB pathways, resulting in a promotion of junctional maturation [29]. With dexamethasone treatment, both lymphatic vessel, blood vessel and blood capillaries (BC) maintained their zipper-like junctions. By contrast, lymphatic capillaries (LC) exhibited “oak-leaf” patterns and started to form button-like structures (Fig. 4C). Quantification of junction structures, defined by Sratio, the external area of cells divided by the internal area of cells (Fig. 4D), produced values ~0.8–1.0 in the presence of VEGF-C in blood capillaries and lymphatic capillaries, indicating an absence of serration at cell-cell boundaries. In contrast, S_{ratio}, in lymphatic capillaries with dexamethasone dropped to ~0.5, indicative of the “zig-zag” structures. Finally, orientation analysis of HUVECs and LECs in the microchannels demonstrated that HUVECs are strongly aligned parallel to the flow direction. Interestingly, LECs were also observed to be aligned, but at 45 degrees relative to the flow direction (Fig. 4D, E).

Anti-angiogenesis drug treatment

To evaluate the potential of this model for drug screening, we treated with three different factors known to inhibit angiogenesis through blockage of VEGF-R1, 2, and 3 (ZM306416, Cabozantinib, and SAR131675, respectively) in the presence of VEGF-A and C (25 ng/ml and 25 ng/ml) in co-culture and mono-culture.

Addition of ZM306416 (antagonist of VEGF-R1) strongly inhibited VA but not LA in co-culture (Fig. 5A, B). Also in co-culture, SAR131675 (antagonist of VEGF-R3) significantly suppressed LA but not VA. This is consistent with expectations since VA is mainly regulated through the VEGF-R1 pathway whereas LA is mainly regulated via the VEGF-R3 pathway. Furthermore, Cabozantinib also inhibited both VA and LA to some extent, demonstrating that VA and LA are induced not only through VEGF-R1 and VEGF-R3 signaling but also by VEGF-R2 signaling. Interestingly, we observed several significant differences between co-culture and mono-culture in terms of sprouting (Fig. 5C). First, SAR131675 (antagonist of VEGF-R3) suppressed LA while having minimal efficacy for impeding VA as in the case of co-culture, although it completely prevented LA under mono-culture conditions, likely due to lymphangiogenesis being primarily regulated by activation of the VEGF-C pathway [31]. These results suggest that VA of HUVECs also affects surrounding LA of LECs. Second, Cabozantinib has minimal potential to inhibit either VA and LA in monoculture, although, in co-culture, Cabozantinib effectively prevents both LA and VA. Finally, there is no significant

difference in the response to ZM306416 between co-culture and monoculture. This result suggests that LA does not influence VA of the neighboring HUVECs.

Relationship between MMP secretion, lymphangiogenesis, and vascular angiogenesis

To investigate possible interactions between LA and VA in co-culture, we focused on MMP activity. MMP array data showed that both HUVECs and LECs secrete various MMPs, especially MMP-1, 2, 3, 9, and 10 (Fig. 6A, B, and C). We also found, however, that LECs secrete significantly less MMPs than HUVECs, especially MMP-2 and 9 (Fig. 6D, E), and that MMP secretion – especially MMP-1, 3, and 10 – is elevated in co-culture compared to monoculture (Fig. 6A- C). To characterize collagen structures after co-culture, matrix fibers were visualized by reflection confocal microscopy (Fig. 6F). The density of collagen fiber of the three conditions (lymphatic vessel + blood vessel, lymphatic vessel + lymphatic vessel, blood vessel + blood vessel) decreased after 7 days of culture compared to control (D0). In particular, collagen structure in co-culture conditions was significantly remodeled to a lower density fiber structure, indicating that co-culture accelerated MMP-1, 3, 9 secretions along with remodeling of the microenvironment, presumably by the combined effects of secretion of new matrix components as well as stresses due to cell contractility.

In addition to the effects of MMP-1, 3, and 10, our results show that HUVECs secrete more MMP-2 and 9 than LEC, resulting in a sequential process in which LA lags behind VA. Consequently, previous studies reported that MMP-2 and MMP-9 are produced by LECs [32, 33]. The secretion of MMP-2 and 9 mainly influence basement membranes of vessel structures and also play a critical role in angiogenesis and lymphangiogenesis. To test these theories further, we applied inhibitors of MMP-2 and MMP-9 to both VA and LA models in the presence of VEGF-A and VEGF-C and found significant reductions in both VA and LA (Fig. 7A and B).

Discussion

Co-cultured and perfusable lymphatic and blood vessels in a microdevice have tremendous potential to facilitate the investigation of interactions between VECs and LECs either in sprouts or mature, large-diameter vessels. Sprout length of LEC did not significantly respond to the addition of VEGF-A, although VEGF-C treatment significantly improved lymphangiogenesis (Supplementary Fig. S1). These results are consistent with numerous previous findings that LECs are mainly regulated by the VEGF-C/VEGFR3 pathway [34] [35] [36], even though they are also stimulated via VEGF-A/VEGFR2 signaling [37] [38] [39] which is limited in LA. Furthermore, we found that LA is often delayed relative to VA in this *in vitro* model. These findings are consistent with *in vivo* behavior during cornea inflammation [40] and tumorigenesis [41] [42].

Perfusion and the associated shear stress through vessel structures has been widely shown to be an important mechanical stimulation, and key to mimicking *in vivo* conditions. Indeed, recent studies have broadly demonstrated that LECs are exquisitely sensitive to mechanical stimulation and that flow plays an important role in lymphatic development [43], valve formation [44] and stabilization of vessels [45]. Increased expression of Prox-1 and ORAI1 (Fig. 2E), especially, has been implicated in the response of lymphatic vessels to mechanical

stimulation [44] and is known to regulate the expression of VEGF-R3 [46] and FGFR-3 [47]. In addition, perfusion culture causes cell alignment of VECs and LECs in the microchannels (Fig. 4). It is well known that VECs typically align with the flow direction as a consequence of shear stress in order to strength the cell-cell junctions and stabilize vessel structures [48] [49]. Lymphatics exhibit similar cell alignment behavior, but over a different range of shear stresses [50]. This result confirms that LEC also sense and respond to shear stress, but the response is different from that of VEC [51]. Therefore, we expect that shear stress by active and passive flow through 3D lumens of blood and lymphatic vessels to be essential to the formation of normal structure, and thus perfusion culture should be necessary to mimic physiological conditions in both types of vessel.

Lymphatic capillaries induced by LA with dexamethasone were observed to exhibit an “oak-leaf” structure with button-like junctions (Fig. 4C). Under physiological conditions, both larger blood vessels and capillaries formed homogeneous tight junctions along the entire boundary of cells, required for low permeability [52]. On the other hand, physiological lymphatic vessels, especially lymphatic capillaries, exhibit a unique junction morphology, which has numerous small gaps between junctions that act as valves that can regulate the passage of immune cells, proteins and interstitial fluid – these are termed *button-like* structures. Transitions between zipper and button junctions are, in fact, key events in controlling lymphatic homeostasis. Judging from our results, lymphatic capillary sprouts formed zipper-like structures because VEGF-C/VEGF-R3 signaling induced an inflammatory response due to the high concentrations of VEGF. In addition, dexamethasone treatment induced transformation to button-like junctions [53]. These results strongly suggest that this *in vitro* model also can be applied to investigate these interactive transformations as mediated by a biological event such as viral infection [54].

Our LA and VA models might be also used to screen for drugs that would effectively prevent diseases associated to VA and LA, such as the dissemination of cancer cells or corneal inflammation, by the addition of culture medium treated with specific antagonists (Figs. 3 and 5). In the present study, treatment with an antagonist of the various VEGFs revealed several important findings. We found that VA precedes and upregulates LA in a co-culture model. Moreover, based on measurements of MMP activity (Fig. 6A-C) and the remodeling of the extracellular matrix after perfusion culture (Fig. 6F), we concluded that communication through MMP regulation is what drives inhibition of VA by LA and helps to explain why inhibition of LA does not prevent VA in co-culture conditions. These results suggest that ECM degradation via MMP-1, 3, and 10 is strongly upregulated by VA in our co-culture model. These MMPs are related to the degradation of collagen type I, II, and III, which is a major comportment of ECM, accelerating LA and VA.

Furthermore, MMP-2 and 9 play an important role in remodeling basement membrane of vessel structures such as collagen type IV, aiding VA followed by LA. This phenomenon appears to be consistent with the pathological interactions of VA and LA [10, 11]. For instance, in the case of corneal inflammation, LA and VA were induced and lymphatic and blood vessels invaded this normally avascular region, resulting in protein deposition, corneal opacity and poor vision [55]. Our models simulate this pathological condition and suggest that the observed induction might be caused in part by enhanced MMP-2 and MMP-9

secretion, leading to changes in the local microenvironment (Fig. 6A-E). Consistent with this, inhibition of MMP-2/MMP-9 activity suppressed both VA and LA, an effect that has been reported *in vivo* [56]. Other studies have also shown that VEGF-A, which is known to induce VA, also stimulates LA [57] and hemangiogenesis via macrophage recruitment [58]. Therefore, our results indicated that not only is the inhibition of VEGF-R1 (VEGF-A) and VEGFR-3 (VEGF-C) important, but also that MMP-2, MMP-9 and other types of MMP should be controlled when investigating anti-LA drugs for cancer metastasis and corneal inflammation (Fig. 7A and B). Thus, preventing degradation of the ECM (e.g., collagen type I) and the basement membrane (e.g., collagen type IV) and/or other matrix components also play an important role in VA and LA.

An obvious application of this model would be in the study of cancer cell intravasation in metastasis. For example, it could be used to characterize the selectivity of different cancer types to enter the vascular or lymphatic circulations. A recent study showed that vascular capillaries and lymphatic capillaries grown in vitro, form independent networks that are not connected to each other in 3D culture, despite the fact that VEC and LEC have similar cell-membrane proteins (e.g. VE-cadherin and PECAM-1) [59]. Our fluorescent images also suggest that vascular and lymphatic capillaries are not connected to each other (Fig. 3F, supplementary Fig. 3 and supplementary movie.1), and result in the formation of individual networks. Further confirmation is needed, however, to demonstrate the absence of connectivity between the lymphatic and vascular capillary beds, such as by perfusion of fluorescent beads through the networks in our model.

Finally, this co-culture model has future potential for the creation of models for metastatic cancer and pathologies with aberrant vascularization, and potentially for drug screening. In such applications, other cell types, such as tumor or immune cells, could be added either to the matrix or the vessels, in order to create a more realistic, tissue-specific model (see e.g., Chen et al, Nat Prot) [60].

Conclusions

In this paper, we demonstrate the fabrication and use of a co-culture platform containing an adjacent lymphatic and vascular structures in which to study lymphangiogenesis and vascular angiogenesis under perfusion conditions. Co-induction of LA and VA showed that VA is followed by LA in the presence of PMA, VEGF-A, and VEGF-C. LA was stimulated by not only VEGF-C but also VEGF-A. Moreover, we demonstrated the effects of antagonists of VEGF-A, B, and C as potential anti-LA and anti-VA drugs. We found that under co-culture conditions, the addition of VEGF-R3 antagonist was reduced in its ability to suppress LA compared to the monoculture condition. These results suggested that VA is also influenced LA. This can be explained in part by the secretion of MMPs by the endothelial cells during VA. This model could help to facilitate the study of pathological responses involving VA and LA such as inflammation, tumorigenesis, and viral infection.

Supplementary Material

Refer to Web version on PubMed Central for supplementary material.

Acknowledgments

T.O. was supported by research fellow overseas (Japan Society for the promotion of science). J.C.S. was supported by the National Science Foundation Graduate Research Fellowship. T.O., J.C.S., and R.D.K and also acknowledge the support of National Science Foundation for a Science and Technology Center on Emergent Behaviors of Integrated Cellular Systems, (CBET-0939511).

References

1. Carmeliet P, Jain RK. Angiogenesis in cancer and other diseases. Nature. 2000; 407(6801):249–57. [PubMed: 11001068]
2. Tammela T, Alitalo K. Lymphangiogenesis: Molecular mechanisms and future promise. Cell. 2010; 140(4):460–76. DOI: 10.1016/j.cell.2010.01.045 [PubMed: 20178740]
3. Cursiefen C, Chen L, Dana MR, Streilein JW. Corneal lymphangiogenesis: evidence, mechanisms, and implications for corneal transplant immunology. Cornea. 2003; 22(3):273–81. [PubMed: 12658100]
4. Ling SQ, Liu C, Li WH, Xu JG, Kuang WH. Corneal lymphangiogenesis correlates closely with hemangiogenesis after keratoplasty. Int J Ophthalmol. 2010; 3(1):76–9. DOI: 10.3980/j.issn. 2222-3959.2010.01.18 [PubMed: 22553523]
5. Bock F, Onderka J, Dietrich T, Bachmann B, Kruse FE, Paschke M, et al. Bevacizumab as a potent inhibitor of inflammatory corneal angiogenesis and lymphangiogenesis. Invest Ophth Vis Sci. 2007; 48(6):2545–52. DOI: 10.1167/iovs.06-0570
6. Bucher F, Parthasarathy A, Bergua A, Onderka J, Regenfuss B, Cursiefen C, et al. Topical Ranibizumab inhibits inflammatory corneal hem- and lymphangiogenesis. Acta Ophthalmol. 2014; 92(2):143–8. DOI: 10.1111/j.1755-3768.2012.02525.x [PubMed: 22994268]
7. Risau W. Mechanisms of angiogenesis. Nature. 1997; 386(6626):671–4. [PubMed: 9109485]
8. Karamysheva AF. Mechanisms of angiogenesis. Biochemistry (Moscow). 2008; 73(7):751.doi: 10.1134/S0006297908070031 [PubMed: 18707583]
9. Papetti M, Herman IM. Mechanisms of normal and tumor-derived angiogenesis. American Journal of Physiology - Cell Physiology. 2002; 282(5):C947–C70. DOI: 10.1152/ajpcell.00389.2001 [PubMed: 11940508]
10. Mimura T, Amano S, Usui T, Kaji Y, Oshika T, Ishii Y. Expression of Vascular Endothelial Growth Factor C and Vascular Endothelial Growth Factor Receptor 3 in Corneal Lymphangiogenesis. Experimental Eye Research. 2001; 72(1):71–8. . DOI: 10.1006/exer.2000.0925 [PubMed: 11133184]
11. Regenfuss B, Bock F, Cursiefen C. Corneal angiogenesis and lymphangiogenesis. Curr Opin Allergy Clin Immunol. 2012; 12(5):548–54. DOI: 10.1097/ACI.0b013e328357b4a2 [PubMed: 22951910]
12. Jeong H-S, Jones D, Liao S, Wattson DA, Cui CH, Duda DG, et al. Investigation of the Lack of Angiogenesis in the Formation of Lymph Node Metastases. JNCI: Journal of the National Cancer Institute. 2015; 107(9) djv155-djv. doi: 10.1093/jnci/djv155
13. Davis GE, Senger DR. Endothelial Extracellular Matrix. Biosynthesis, Remodeling, and Functions During Vascular Morphogenesis and Neovessel Stabilization. 2005; 97(11):1093–107. DOI: 10.1161/01.RES.0000191547.64391.e3
14. Donovan D, Brown NJ, Bishop ET, Lewis CE. Comparison of three in vitro human 'angiogenesis' assays with capillaries formed in vivo. Angiogenesis. 2001; 4(2):113–21. DOI: 10.1023/a: 1012218401036 [PubMed: 11806243]
15. Baker M, Robinson SD, Lechertier T, Barber PR, Tavora B, D'Amico G, et al. Use of the mouse aortic ring assay to study angiogenesis. Nat Protocols. 2012; 7(1):89–104. http://www.nature.com/nprot/iournal/v7/n1/abs/nprot.2011.435.html#supplementarv-information.
16. Nguyen D-HT, Stapleton SC, Yang MT, Cha SS, Choi CK, Galie PA, et al. Biomimetic model to reconstitute angiogenic sprouting morphogenesis in vitro. Proceedings of the National Academy of Sciences. 2013; 110(17):6712–7. DOI: 10.1073/pnas.1221526110

17. Heiss M, Hellstrom M, Kalen M, May T, Weber H, Hecker M, et al. Endothelial cell spheroids as a versatile tool to study angiogenesis in vitro. FASEB J. 2015; 29(7):3076–84. DOI: 10.1096/fj.14-267633 [PubMed: 25857554]

18. Nehls V, Drenckhahn D. A Novel, Microcarrier-Based in Vitro Assay for Rapid and Reliable Quantification of Three-Dimensional Cell Migration and Angiogenesis. Microvascular Research. 1995; 50(3):311–22. . DOI: 10.1006/mvre.1995.1061 [PubMed: 8583947]

19. Kim S, Lee H, Chung M, Jeon NL. Engineering of functional, perfusable 3D microvascular networks on a chip. Lab on a Chip. 2013; 13(8):1489–500. DOI: 10.1039/C3LC41320A [PubMed: 23440068]

20. Choi D, Park E, Jung E, Seong YJ, Yoo J, Lee E, et al. Laminar flow downregulates Notch activity to promote lymphatic sprouting. The Journal of clinical investigation. 2017; 127(4):1225–40. DOI: 10.1172/JCI87442 [PubMed: 28263185]

21. Kim S, Chung M, Jeon NL. Three-dimensional biomimetic model to reconstitute sprouting lymphangiogenesis in vitro. Biomaterials. 2016; 78:115–28. . DOI: 10.1016/i.biomaterials.2015.11.019 [PubMed: 26691234]

22. Chung M, Ahn J, Son K, Kim S, Jeon NL. Biomimetic Model of Tumor Microenvironment on Microfluidic Platform. Adv Healthc Mater. 2017; doi: 10.1002/adhm.201700196

23. Stacker SA, Williams SP, Karnezis T, Shayan R, Fox SB, Achen MG. Lymphangiogenesis and lymphatic vessel remodelling in cancer. Nat Rev Cancer. 2014; 14(3):159–72. DOI: 10.1038/nrc3677 [PubMed: 24561443]

24. Kawai Y, Hosaka K, Kaidoh M, Minami T, Kodama T, Ohhashi T. Heterogeneity in Immunohistochemical, Genomic, and Biological Properties of Human Lymphatic Endothelial Cells Between Initial and Collecting Lymph Vessels. Lymphatic Research and Biology. 2008; 6(1):15–27. DOI: 10.1089/lrb.2007.1019 [PubMed: 18361767]

25. Montesano R, Orci L. Phorbol esters induce angiogenesis in vitro from large-vessel endothelial cells. J Cell Physiol. 1987; 130(2):284–91. DOI: 10.1002/jcp.1041300215 [PubMed: 2434516]

26. Osaki T, Kakegawa T, Kageyama T, Enomoto J, Nittami T, Fukuda J. Acceleration of Vascular Sprouting from Fabricated Perfusable Vascular-Like Structures. PLOS ONE. 2015; 10(4):e0123735.doi: 10.1371/journal.pone.0123735 [PubMed: 25860890]

27. Hume SL, Hoyt SM, Walker JS, Sridhar BV, Ashley JF, Bowman CN, et al. Alignment of multi-layered muscle cells within three-dimensional hydrogel macrochannels. Acta Biomaterialia. 2012; 8(6):2193–202. https://doi.ore/10.1016/i.actbio.2012.02.001. [PubMed: 22326973]

28. Morimoto Y, Kato-Negishi M, Onoe H, Takeuchi S. Three-dimensional neuron-muscle constructs with neuromuscular junctions. Biomaterials. 2013; 34(37):9413–9. DOI: 10.1016/j.biomaterials.2013.08.062 [PubMed: 24041425]

29. Yao L-C, Baluk P, Srinivasan RS, Oliver G, McDonald DM. Plasticity of Button-Like Junctions in the Endothelium of Airway Lymphatics in Development and Inflammation. The American journal of pathology. 2012; 180(6):2561–75. . DOI: 10.1016/i.aipath.2012.02.019 [PubMed: 22538088]

30. Baluk P, Fuxe J, Hashizume H, Romano T, Lashnits E, Butz S, et al. Functionally specialized junctions between endothelial cells of lymphatic vessels. The Journal of Experimental Medicine. 2007; 204(10):2349–62. DOI: 10.1084/jem.20062596 [PubMed: 17846148]

31. Hirakawa S, Brown LF, Kodama S, Paavonen K, Alitalo K, Detmar M. VEGF-C-induced lymphangiogenesis in sentinel lymph nodes promotes tumor metastasis to distant sites. Blood. 2007; 109(3):1010–7. DOI: 10.1182/blood-2006-05-021758 [PubMed: 17032920]

32. Bruyere F, Melen-Lamalle L, Blacher S, Roland G, Thiry M, Moons L, et al. Modeling lymphangiogenesis in a three-dimensional culture system. Nature methods. 2008; 5(5):431–7. DOI: 10.1038/nmeth.1205 [PubMed: 18425139]

33. Nakamura ES, Koizumi K, Kobayashi M, Saiki I. Inhibition of lymphangiogenesis-related properties of murine lymphatic endothelial cells and lymph node metastasis of lung cancer by the matrix metalloproteinase inhibitor MMI270. Cancer Sci. 2004; 95(1):25–31. [PubMed: 14720323]

34. Onimaru M, Yonemitsu Y, Fujii T, Tanii M, Nakano T, Nakagawa K, et al. VEGF-C regulates lymphangiogenesis and capillary stability by regulation of PDGF-B. Am J Physiol Heart Circ Physiol. 2009; 297(5):H1685–96. DOI: 10.1152/ajpheart.00015.2009 [PubMed: 19734356]

35. Szuba A, Skobe M, Karkkainen MJ, Shin WS, Beynet DP, Rockson NB, et al. Therapeutic lymphangiogenesis with human recombinant VEGF-C. FASEB J. 2002; 16(14):1985–7. DOI: 10.1096/fj.02-0401fje [PubMed: 12397087]
36. Wang XL, Zhao J, Qin L, Qiao M. Promoting inflammatory lymphangiogenesis by vascular endothelial growth factor-C (VEGF-C) aggravated intestinal inflammation in mice with experimental acute colitis. Braz J Med Biol Res. 2016; 49(5):e4738.doi: 10.1590/1414-431X20154738 [PubMed: 27074165]
37. Halin C, Tobler NE, Vigl B, Brown LF, Detmar M. VEGF-A produced by chronically inflamed tissue induces lymphangiogenesis in draining lymph nodes. Blood. 2007; 110(9):3158–67. DOI: 10.1182/blood-2007-01-066811 [PubMed: 17625067]
38. Mallory BP, Mead TJ, Wiginton DA, Kulkarni RM, Greenberg JM, Akeson AL. Lymphangiogenesis in the developing lung promoted by VEGF-A. Microvasc Res. 2006; 72(1–2): 62–73. DOI: 10.1016/j.mvr.2006.05.002 [PubMed: 16806288]
39. Kadowaki I, Ichinohasama R, Harigae H, Ishizawa K, Okitsu Y, Kameoka J, et al. Accelerated lymphangiogenesis in malignant lymphoma: possible role of VEGF-A and VEGF-C. Br J Haematol. 2005; 130(6):869–77. DOI: 10.1111/j.1365-2141.2005.05695.x [PubMed: 16156857]
40. Cursiefen C, Seitz B, Dana MR, Streilein JW. Angiogenesis and lymphangiogenesis in the cornea. Pathogenesis, clinical implications and treatment options. Ophthalmologe. 2003; 100(4):292–9. DOI: 10.1007/s00347-003-0798-y [PubMed: 12682761]
41. Paduch R. The role of lymphangiogenesis and angiogenesis in tumor metastasis. Cell Oncol (Dordr). 2016; 39(5):397–410. DOI: 10.1007/s13402-016-0281-9 [PubMed: 27126599]
42. Foubert P, Varner JA. Integrins in tumor angiogenesis and lymphangiogenesis. Methods in molecular biology. 2012; 757:471–86. DOI: 10.1007/978-1-61779-166-6_27 [PubMed: 21909928]
43. Planas - Paz L, Strilic B, Goedecke A, Breier G, Fassler R, Lammert E. Mechanoinduction of lymph vessel expansion. The EMBO Journal. 2012; 31(4):788–804. DOI: 10.1038/emboj.2011.456 [PubMed: 22157817]
44. Sabine A, Agalarov Y, Maby-El Hajjami H, Jaquet M, Hâgerling R, Pollmann C, et al. Mechanotransduction, PROX1, and FOXC2 Cooperate to Control Connexin37 and Calcineurin during Lymphatic-Valve Formation. Developmental Cell. 2012; 22(2):430–45. . DOI: 10.1016/i.devcel.2011.12.020 [PubMed: 22306086]
45. Sweet DT, Jiménez JM, Chang J, Hess PR, Mericko-Ishizuka P, Fu J, et al. Lymph flow regulates collecting lymphatic vessel maturation in vivo. The Journal of clinical investigation. 2015; 125(8): 2995–3007. DOI: 10.1172/JCI79386 [PubMed: 26214523]
46. Pan M-R, Chang T-M, Chang H-C, Su J-L, Wang H-W, Hung W-C. Sumoylation of Prox1 controls its ability to induce VEGFR3 expression and lymphatic phenotypes in endothelial cells. J Cell Sci. 2009; 122(18):3358–64. DOI: 10.1242/jcs.050005 [PubMed: 19706680]
47. Shin JW, Min M, Larrieu-Lahargue F, Canron X, Kunstfeld R, Nguyen L, et al. Prox1 promotes lineage-specific expression of fibroblast growth factor (FGF) receptor-3 in lymphatic endothelium: A role for FGF signaling in lymphangiogenesis. Mol Biol Cell. 2006; 17(2):576–84. DOI: 10.1091/mbc.E05-04-0368 [PubMed: 16291864]
48. Wang C, Baker BM, Chen CS, Schwartz MA. Endothelial cell sensing of flow direction. Arteriosclerosis, thrombosis, and vascular biology. 2013; 33(9)doi: 10.1161/ATVBAHA.113.301826
49. Seiichi O, Susumu I, Yukio Y. Alignment of vascular endothelial cells as a collective response to shear flow. Journal of Physics D: Applied Physics. 2015; 48(24):245401.
50. Baeyens N, Nicoli S, Coon BG, Ross TD, Van den Dries K, Han J, et al. Vascular remodeling is governed by a VEGFR3-dependent fluid shear stress set point. eLife. 2015; 4:e04645.doi: 10.7554/eLife.04645
51. Chiu J-J, Chien S. Effects of Disturbed Flow on Vascular Endothelium: Pathophysiological Basis and Clinical Perspectives. Physiological Reviews. 2011; 91(1):327–87. DOI: 10.1152/physrev.00047.2009 [PubMed: 21248169]
52. Wallez Y, Huber P. Endothelial adherens and tight junctions in vascular homeostasis, inflammation and angiogenesis. Biochimica et Biophysica Acta (BBA) - Biomembranes. 2008; 1778(3):794–809. . DOI: 10.1016/j.bbamem.2007.09.003 [PubMed: 17961505]

53. Greco KV, Lara PF, Oliveira-Filho RM, Greco RV, Sudo-Hayashi LS. Lymphatic regeneration across an incisional wound: inhibition by dexamethasone and aspirin, and acceleration by a micronized purified flavonoid fraction. Eur J Pharmacol. 2006; 551(1–3):131–42. DOI: 10.1016/j.ejphar.2006.08.090 [PubMed: 17045986]

54. Bryant-Hudson KM, Gurung HR, Zheng M, Carr DJJ. Tumor Necrosis Factor Alpha and Interleukin-6 Facilitate Corneal Lymphangiogenesis in Response to Herpes Simplex Virus 1 Infection. Journal of virology. 2014; 88(24):14451–7. DOI: 10.1128/Jvi.01841-14 [PubMed: 25297992]

55. Patel SP, Dana R. Corneal lymphangiogenesis: implications in immunity. Semin Ophthalmol. 2009; 24(3):135–8. DOI: 10.1080/08820530902801320 [PubMed: 19437348]

56. Du HT, Du LL, Tang XL, Ge HY, Liu P. Blockade of MMP-2 and MMP-9 inhibits corneal lymphangiogenesis. Graefes Arch Clin Exp Ophthalmol. 2017; 255(8):1573–9. DOI: 10.1007/s00417-017-3651-8 [PubMed: 28669039]

57. Hirakawa S, Kodama S, Kunstfeld R, Kajiya K, Brown LF, Detmar M. VEGF-A induces tumor and sentinel lymph node lymphangiogenesis and promotes lymphatic metastasis. J Exp Med. 2005; 201(7):1089–99. DOI: 10.1084/jem.20041896 [PubMed: 15809353]

58. Cursiefen C, Chen L, Borges LP, Jackson D, Cao J, Radziejewski C, et al. VEGF-A stimulates lymphangiogenesis and hemangiogenesis in inflammatory neovascularization via macrophage recruitment. The Journal of clinical investigation. 2004; 113(7):1040–50. DOI: 10.1172/JCI20465 [PubMed: 15057311]

59. Matsusaki M, Case CP, Akashi M. Three-dimensional cell culture technique and pathophysiology. Advanced Drug Delivery Reviews. 2014; 74(Supplement C):95–103. . DOI: 10.1016/i.addr.2014.01.003 [PubMed: 24462454]

60. Chen MB, Whisler JA, Frose J, Yu C, Shin Y, Kamm RD. On-chip human microvasculature assay for visualization and quantification of tumor cell extravasation dynamics. Nat Protocols. 2017; 12(5):865–80. http://www.nature.com/nprot/iournal/v12/n5/abs/nprot.2017.018.html#supplementarv-information. DOI: 10.1038/nprot.2017.018 [PubMed: 28358393]

Lay summary

Lymphangiogenesis involves the formation of new lymphatic vessels from pre-existing ones during embryonic development, wound healing and in various pathological conditions. In this work, we simulate such physiological and pathological conditions in which there are important bidirectional effects between the lymphatic and vascular cells using an *in vitro* perfusion culture. Mechanical and chemical stimuli *in vitro* lead to maturation of the lymphatic structures as evidenced by lymphatic-specific cell-cell junctions and cell orientation. The combined vascular and lymphatic angiogenesis model could be useful to investigate the pathophysiology of tumorigenesis and corneal inflammation involving interactions between vascular angiogenesis and lymphatic angiogenesis.

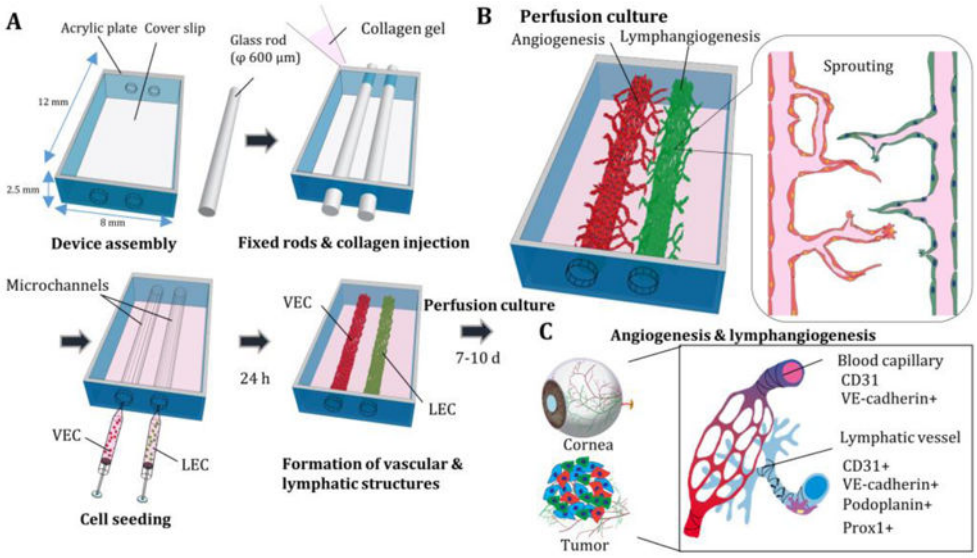

Fig. 1. Schematic illustration of engineered lymphatic and vascular structures

(A) Acrylic plates and glass coverslip were assembled and glass rods were fixed in the culture chamber. Then, collagen gel was added and placed in an incubator for 15 min. After extraction of glass rods, cell suspensions of vascular endothelial cells (VEC) and lymphatic endothelial cells (LEC) were injected into the microchannels. After 24 h of static culture, a peristaltic pump was connected to both vessels to maintain a perfusion culture for 7-10 day and lymphangiogenesis and angiogenesis were observed (B). (C) Characterizations of lymphangiogenesis (LA) and vascular angiogenesis (VA) in cornea injury and tumorigenesis.

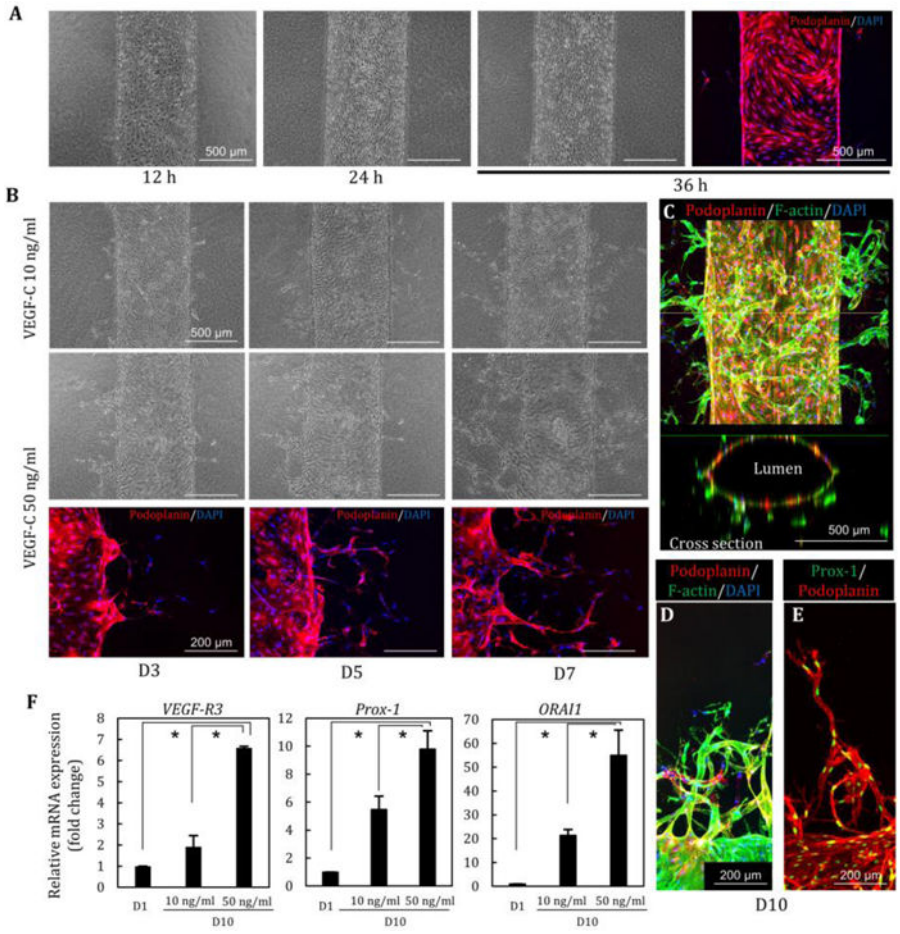

Fig. 2. Lymphatic vessel structures and lymphangiogenesis induced by VEGF-C

(A) Lymphatic endothelial cells (LECs) were adhered to microchannels in 12 h, resulting in the formation of the lymphatic vessel in 24–36h. (B) Lymphatic morphogenesis was induced in a dose-dependent manner of VEGF-C (10, 50 ng/ml) at D3, D5, and D7. Podoplanin was expressed in lymphatic angiogenic sprouting. (C) Lumen structure of lymphatic vessel after 10 days of perfusion culture. (D, E) Lymphatic sprouting and single cell migration stained by podoplanin and Prox-1. (F) Relative gene expression changes at D1 and D10 (VEGF-C 10 and 50 ng/ml). High concentration of VEGF-C induces increasing the expression of VEGF-R3, Prox1, and ORAI1. *, $p<0.01$, error bar=±SD.

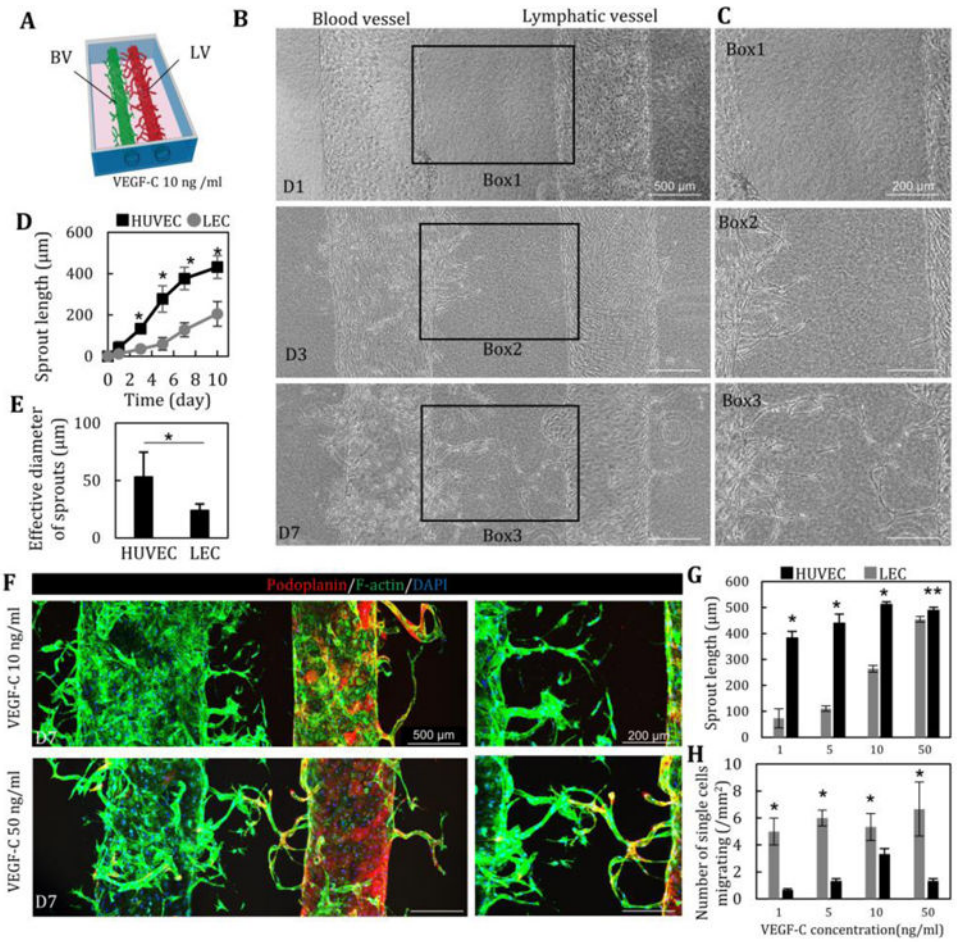

Fig. 3. Lymphatic and blood vessel structures in a collagen matrix

(A, B) LA and VA were induced by the addition of VEGF-C (10 ng/ml). HUVEC started to migrate and sprout into collagen gel at D3, prior to LEC sprouting. (C) Quantitative comparison of sprouting length (D) and effective diameter (E) of HUVEC and LEC. n=12. LA lagged behind VA. (F) Immunostaining of podoplanin (red) and F-actin (green) and nuclear (blue) of LA and VA at D7 at 10 and 50 ng/ml of VEGF-C. (G) Enhancement of LA and VA at D7 in a dose-dependent manner of VEGF-C (1, 5, 10 and 50 ng/ml). n=5. (H) Single cell migration of HUVEC and LEC at D7. n=5. *, $p<0.01$; **, $p<0.05$, error bar= ±SD.

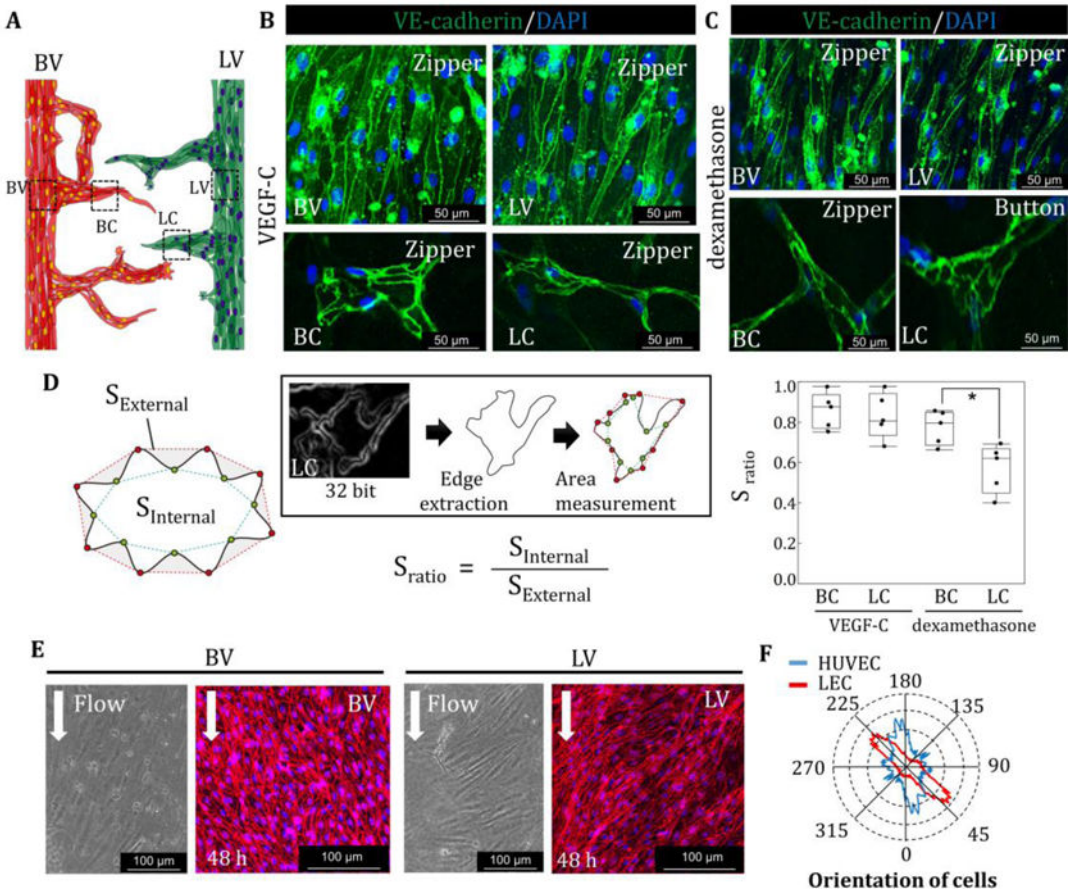

Fig. 4. Cell-cell junctions in blood and lymphatic vessels and orientation of cells

(A) VE-cadherin staining in lymphatic vessel (LV), blood vessel (BV), blood capillaries (BC), and lymphatic capillaries (LC). (B) VE-cadherin was highly expressed at the boundary of cells in the presence of VEGF-C in BV, LV, BC, and LC, forming “zipper-like junctions”. (C) VE-cadherin expression was localized at the cell-cell boundary with dexamethasone only with the addition of VEGF-C at BV and LV. Zipper-like structures formed at BC. In contrast, LC start to take on an “oak-leaf” appearance, resulting in the formation of button-like structures in LC. (D) Sratio is defined by the internal area of cells divided by the external area of cells. LEC in LC formed serrated structures compared to VEC in BC in the presence of dexamethasone. (E) Representative images of cell orientation in the BV and LV and quantification of directionality by FFT (F). *, $p<0.01$, error bar=±SD.

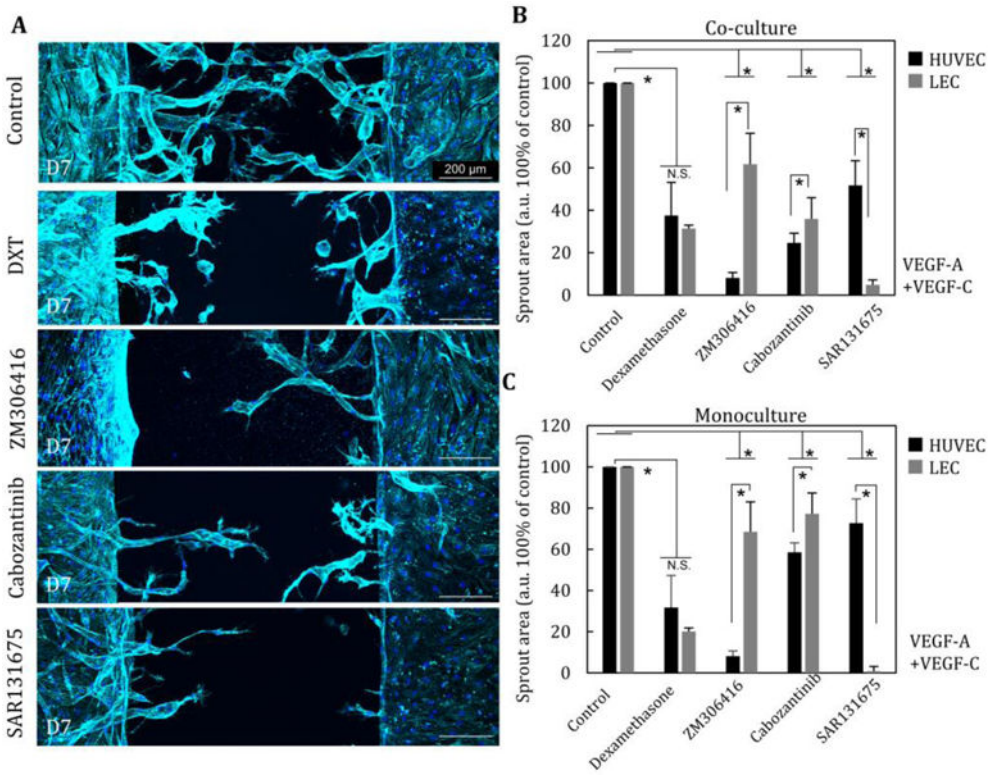

Fig. 5. Inhibition of lymphangiogenesis and vascular angiogenesis

(A) Influence of LA and VA by addition of steroid anti-inflammatory drug (dexamethasone) and selective inhibitors of different VEGF receptors (ZM306416, Cabozantinib, and SAR131675) in the presence of VEGF-A (25 ng/ml), VEGF-C (25 ng/ml). (B) Quantitative comparison of sprouting area at 5 different conditions in co-culture (n=5) and monoculture (n=3) (C). *, $p<0.01$, error bar=±SD.

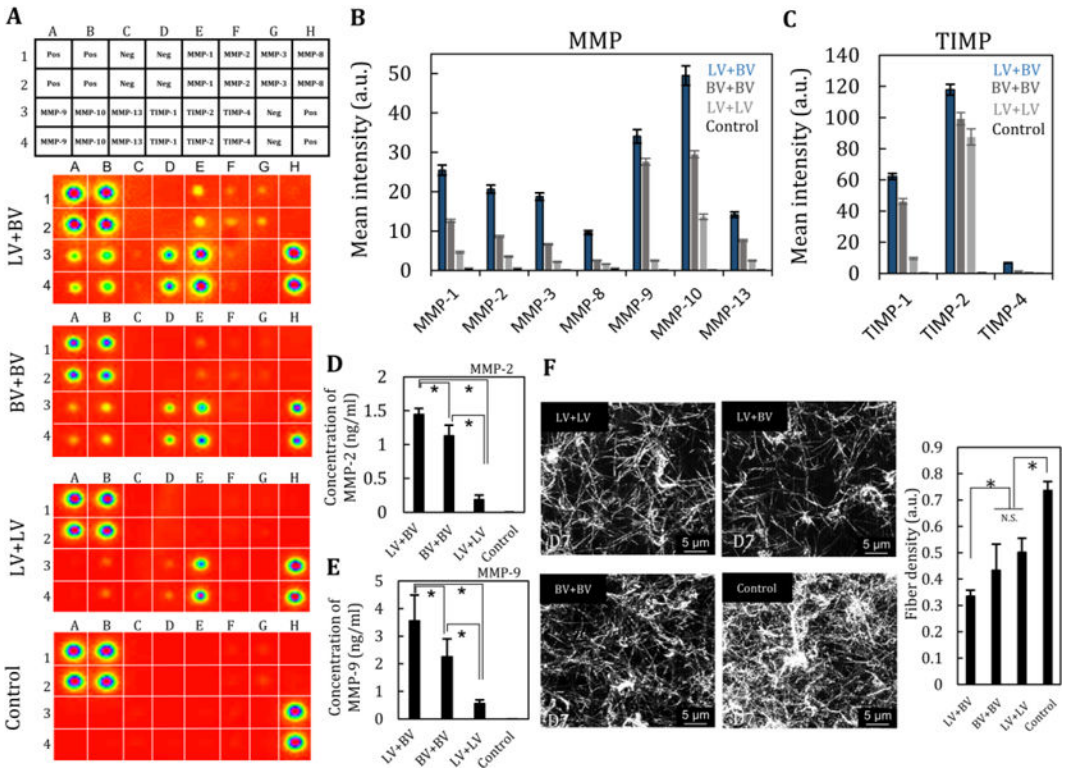

Fig. 6. MMP secretion and degradation of collagen by lymphangiogenesis and angiogenesis

(A) MMP array of exhausted culture medium at D7 in four conditions: lymphatic vessel + blood vessel, blood vessel + blood vessel, lymphatic vessel+ lymphatic vessel, and control (EGM2-MV). n=2. (B) Quantification of MMP concentration and (C) TIMP concentration. (D, E) Quantitative measurement of the concentration of MMP-2 and MMP-9 by ELISA. n=3. (F) Reflectance images of collagen matrix after 7 days of culture and fiber density. n=3. *, $p<0.01$, error bar=±SD.

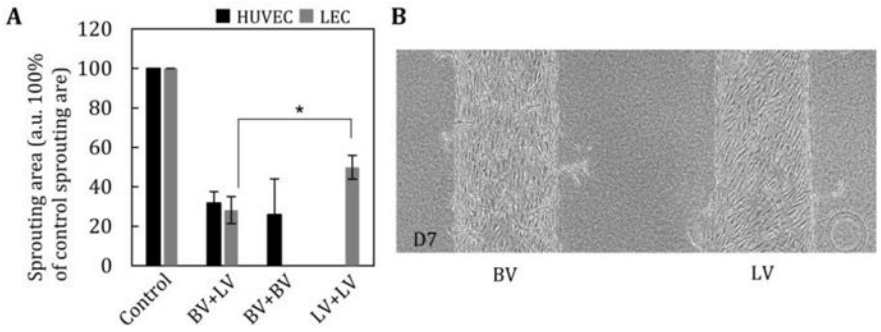

Fig. 7. Addition of an inhibitor of MMP2 and MMP-9 suppresses lymphangiogenesis and vascular angiogenesis

(A) Average sprouting area by addition of an MMP-2/MMP-9 inhibitor. The inhibitor significantly prevented both vascular angiogenesis and lymphatic angiogenesis. n=5. (B) Representative image of blood vessel (BV) and lymphatic vessel (LV) with MMP inhibitor at D7. *, $p<0.01$, error bar=±SD.